Optics Communications 426 (2018) 94–98

Contents lists available at ScienceDirect

Optics Communications

journal homepage: www.elsevier.com/locate/optcom

Underwater wireless optical communication using a lens-free solar panel receiver

Meiwei Kong [a,b], Bin Sun [a,b], Rohail Sarwar [a,b], Jiannan Shen [a,b], Yifei Chen [a,b], Fengzhong Qu [a], Jun Han [c], Jiawang Chen [a], Huawei Qin [d], Jing Xu [a,b,*]

[a] *Key Laboratory of Ocean Observation-Imaging Testbed of Zhejiang Province, Ocean College, Zhejiang University, Zheda Road 1, Zhoushan, Zhejiang, 316021, PR China*
[b] *Optical Communications Laboratory, Ocean College, Zhejiang University, Zheda Road 1, Zhoushan, Zhejiang, 316021, PR China*
[c] *School of Electrical Engineering and Telecommunications, The University of New South Wales, Australia*
[d] *The Institute of Engineering, Hangzhou Dianzi University, Hangzhou, Zhejiang, 310018, PR China*

ARTICLE INFO

Keywords:
Solar panel
OFDM
Underwater wireless optical communication

ABSTRACT

In this paper, we first propose that self-powered solar panels featuring large receiving area and lens-free operation have great application prospect in underwater vehicles or underwater wireless sensor networks (UWSNs) for data collection. It is envisioned to solve the problem of link alignment. The low-cost solar panel used in the experiment has a large receiving area of 5 cm^2 and a receiving angle of 20°. Over a 1-m air channel, a 16-quadrature amplitude modulation (QAM) orthogonal frequency division multiplexing (OFDM) signal at a data rate of 20.02 Mb/s is successfully transmitted within the receiving angle of 20°. Over a 7-m tap water channel, we achieve data rates of 20.02 Mb/s using 16-QAM, 18.80 Mb/s using 32-QAM and 22.56 Mb/s using 64-QAM, respectively. By adding different quantities of $Mg(OH)_2$ powders into the water, the impact of water turbidity on the solar panel-based underwater wireless optical communication (UWOC) is also investigated.

1. Introduction

The ocean, rich in huge untapped natural resources, is bearing great hopes of human beings. Developing underwater vehicles and underwater wireless sensor networks (UWSNs) is an inevitable way to promote the advancement of oceanic research and exploration. Underwater communication systems are indispensable parts of underwater equipment for underwater surveillance and data transmission. Conventional underwater acoustic communication features high reliability and stability, but it suffers limited bandwidth and large propagation delay, which is unable to satisfy certain applications requiring large data volume and high data rate. Alternatively, underwater wireless optical communication (UWOC) with high bandwidth has become a growing research trend in recent years [1–6]. Considering that underwater energy provisioning is one of the burning issues restricting the development of underwater equipment, UWOC with outstanding advantages of small size, light weight and low power consumption makes it a promising choice in underwater platforms and UWSNs. Previous research work mainly focused on stationary point-to-point UWOC with the purpose of increasing underwater transmission rate (up to several Gb/s) or distance [1–6]. Positive–intrinsic–negative (PIN) diodes [1–3] or avalanche photodiodes (APDs) [4–6] are the commonly used photodiodes (PDs). They have small active area, so convex lenses are usually employed to focus light, implying that accurate pointing is required between the transmitter and receiver. However, in practical underwater scenarios, transceiver mobility will make the link alignment very challenging and thus greatly affect the system performance. Moreover, PIN diodes/APDs usually work with biasing circuitries and trans-impedance amplifiers at the receiver side, for which external power supply is required. In fact, there are many situations where one end of the link has very limited power and even has difficulty in battery charge or replacement like the nodes of UWSNs. Such small platforms may have medium data rate requirements (1 to 100 Mb/s). Given the facts above, a solar panel-based receiver, serving the dual purpose of signal detection and energy harvesting in a UWOC system, is an interesting alternative. In recent years, solar panels used as detectors have been preliminarily studied in the field of visible light communication (VLC) [7–11]. They not only can directly convert the optical signal to an electrical signal without external power supply, but can also harvest energy from the direct current (DC) component of the modulated light to power user terminals [7]. In [9], the authors first used an organic semiconductor solar cell, which is flexible enough to be integrated on varieties of devices or substrates, as an energy-harvesting receiver for VLC. A data rate of 34.3 Mb/s

* Corresponding author at: Optical Communications Laboratory, Ocean College, Zhejiang University, Zheda Road 1, Zhoushan, Zhejiang, 316021, PR China.
E-mail address: jxu-optics@zju.edu.cn (J. Xu).

https://doi.org/10.1016/j.optcom.2018.05.019
Received 14 February 2018; Received in revised form 5 May 2018; Accepted 7 May 2018
0030-4018/© 2018 Published by Elsevier B.V.

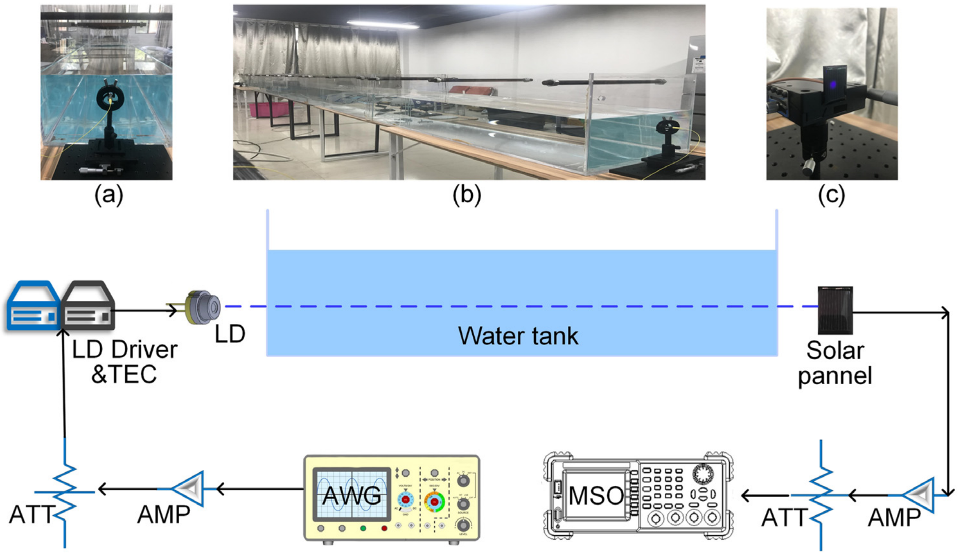

Fig. 1. Experimental setup of the proposed UWOC system using a self-powered solar panel as the detector. Insets: (a) the transmitter module, (b) the water tank, and (c) the low-cost solar panel.

was achieved using orthogonal frequency-division multiplexing (OFDM) over a 1 m air channel. The prior work renders us plentiful inspirations of future underwater equipment using solar panels, many of which could be self-powered with simultaneous wireless data transmission. However, the potential of solar panels with the advantages of large receiving area and lens-free operation, which are expected to availably solve the problem of link alignment, has not been explored.

In this paper, for the first time, we investigate the superiority of a solar panel used as a detector in a UWOC system. Compared with PIN diodes and APDs, the off-the-shelf solar panel we used has a large receiving angle of around 20° and a receiving area of around 5 cm^2, which can relax the requirement on the alignment between the transmitter and receiver. Within the receiving angle of 20°, a 20.02-Mb/s 16-quadrature amplitude modulation (QAM) OFDM signal is successfully transmitted through a 1-m air channel. Over a 7-m tap water channel, data rates of 20.02 Mb/s using 16-QAM, 18.80 Mb/s using 32-QAM and 22.56 Mb/s using 64-QAM are achieved, respectively. $Mg(OH)_2$ powders are gradually added into the water for studying the effect of water turbidity on the solar panel-based UWOC.

2. Experimental setup

Fig. 1 depicts the experimental setup of the proposed UWOC system using a self-powered solar panel as a detector. The transmitter module, the water tank and the low-cost solar panel are presented in the insets. The transmitter was a 30-mW single-mode pigtailed 405-nm LD (Thorlabs LP405-SF30) employing an LD controller and a temperature controller to set the bias current and maintain the temperature, respectively. The optimum bias current was 60 mA and the temperature was stabilized at 25 °C. 16-QAM/32-QAM/64-QAM OFDM signals generated offline and output from an arbitrary waveform generator (AWG) were first transmitted to a 25-dB amplifier (AMP) and a key-press variable electrical attenuator (ATT) to adjust the signal amplitudes. The sampling rate of the AWG was set at 125 MSamples/s in the case of transmitting 16-QAM OFDM signal and 50 MSamples/s in the case of transmitting 32-QAM/64-QAM OFDM signals. Then, the OFDM signals were superposed onto the blue-light LD via an LD and thermoelectric cooler (TEC) mount. The directly modulated light was detected by a cheap off-the-shelf silicon-based solar panel (30 mm long, 25 mm wide), after transmitting through a water tank (7 m long, 0.4 m wide, and 0.4 m high). The water tank was filled with 581.96-L fresh tap water. In the experiment, by mixing scattering agent $Mg(OH)_2$ powders with the water, some

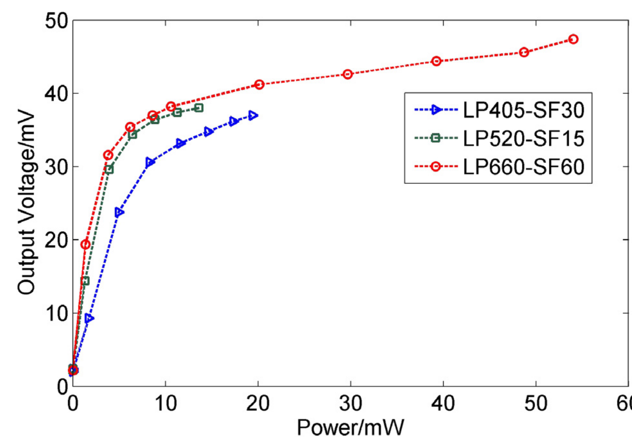

Fig. 2. Sensitivity curves of the solar panel to the 405-nm, 520-nm, and 660-nm light.

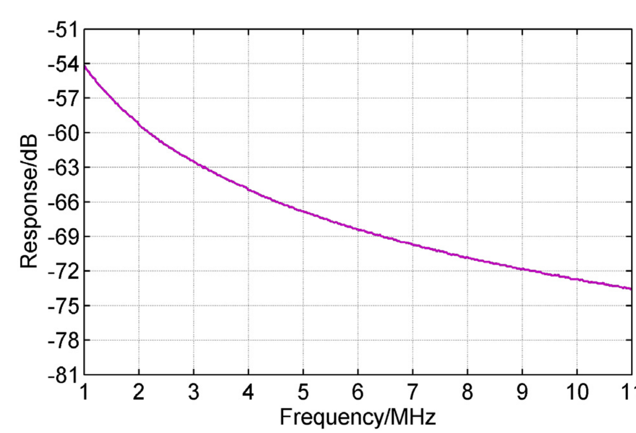

Fig. 3. Back-to-back frequency response of the system employing the 405-nm LD as the transmitter and the solar panel as the detector.

measurements were carried out. The open-circuit voltage and short-circuit current of the solar panel are 1 V and 100 mA, respectively. After

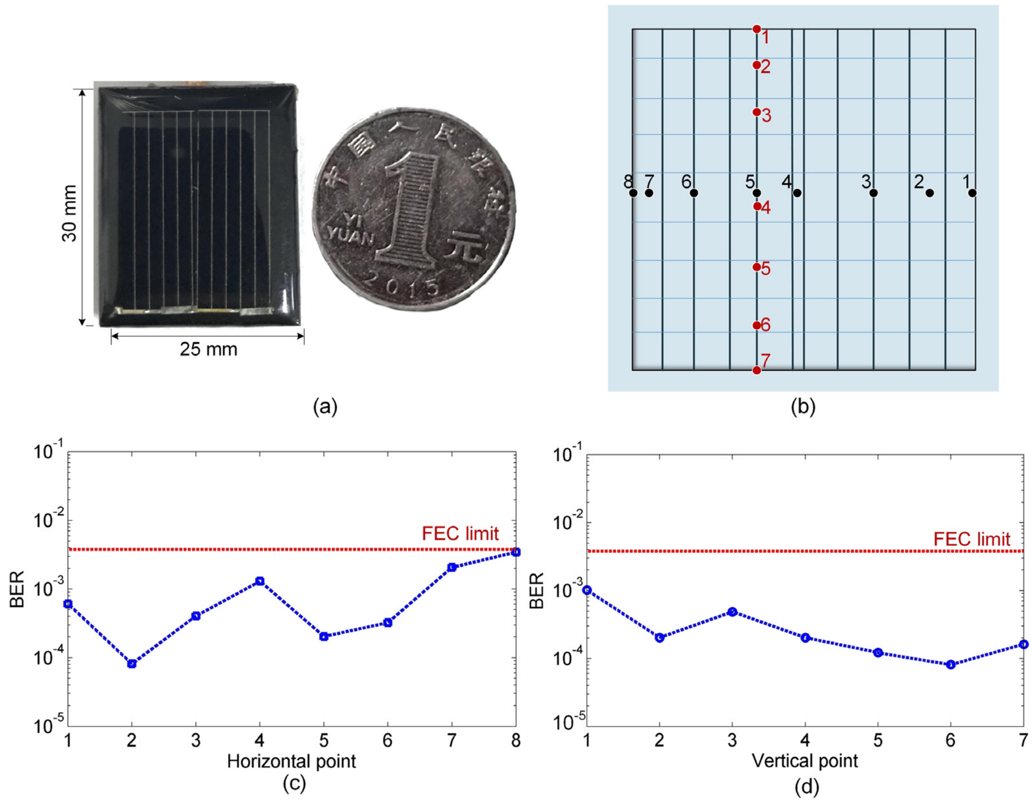

Fig. 4. (a) Solar panel with a 1-yuan RMB coin as a reference. (b) Diagrammatic sketch of the solar panel and measured points. (c) BERs versus horizontal points from 1 to 8. (d) BERs versus vertical points from 1 to 7.

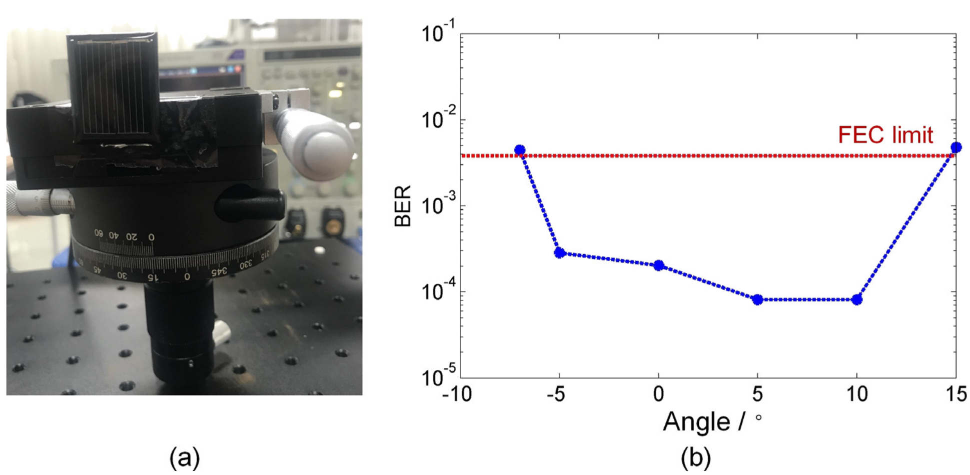

Fig. 5. (a) Receiver module and (b) BERs of the 20.02-Mb/s 16-QAM OFDM signal over a 1-m air channel, when the solar panel is at different angles.

being adjusted by another AMP and ATT, the received OFDM signals were captured by a mixed signal oscilloscope (MSO) with the sampling rate of 1.25 GSamples/s and demodulated offline.

3. Experimental results

We first measured the sensitivity curves of the solar panel to the 405-nm, 520-nm, and 660-nm light. In each measurement, the LD (Thorlabs LP405-SF30, Thorlabs LP520-SF15, or Thorlabs LP660-SF60), a neutral density filter and the solar panel were successively put in close proximity to each other. The laser beam passed through the collimator and vertically illuminated on the solar panel. By adjusting the neutral density filter and the bias current of the LD, different output voltages and optical powers were obtained. From Fig. 2, we can conclude that the solar panel is most sensitive to the 660-nm light, followed by the 520-nm light and the 405-nm light, but the differences among them are not very big. With an input power of less than 5 mW, the response of solar panel is roughly linear. Considering that the 405-nm light has a smaller absorption coefficient in pure water compared with the 520-nm and 660-nm light for UWOC [12], the following experiment was conducted using the 405-nm LD. Then, we set up an experimental system using the 405-nm LD as the transmitter and the solar panel as the detector. The back-to-back frequency response of the system measured by a vector network analyzer is shown in Fig. 3. As the starting frequency of the vector network analyzer is 1 MHz, the 3-dB bandwidth of the system is considered not more than 1.5 MHz. Such a small system bandwidth is attributed to the limited bandwidth of the solar panel.

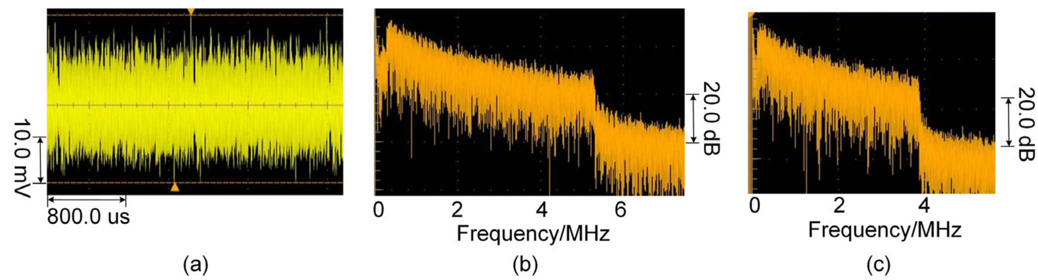

Fig. 6. (a) Waveform and (b) Spectrum of the 20.02-Mb/s 16-QAM OFDM signal. (c) Spectrum of the 22.56-Mb/s 64-QAM OFDM signal.

We tested the communication performance of the solar panel over a 1-m air channel. Using a 16-QAM OFDM signal with 41 subcarriers, we achieved a gross data rate of 20.02 Mb/s (a net bit rate of 16.54 Mb/s). Fig. 4(a) shows the off-the-shelf solar panel (length: 30 mm, width: 25 mm) with a 1-yuan RMB coin as a reference. The receiving area of the solar panel is around 5 cm^2 (length: 25 mm, width: 20 mm). Fig. 4(b) is the diagrammatic sketch of the solar panel including 8 horizontal points and 7 vertical points. These representative points are selected to test BER performances, which are located at the edges, the fingers and the region between two adjacent fingers of the solar panel. The BERs versus horizontal points from 1 to 8 and those versus vertical points from 1 to 7 are illustrated in Fig. 4(c) and (d), respectively. From Fig. 4(c) and (d), we can conclude that the impact of fingers of the solar panel on the BER performances are not very serious. However, the BERs were a bit higher at vertical point 1 and horizontal points 1, 4, 7 and 8, locating at the edges of the low-cost solar panel. It indicates that the communication performances at the edge of the solar panel are not very good due to the manufacturing technique. In the following experiment, we did not use these points for data transmission.

As the solar panel has a large receiving area of 5 cm^2 to receive sufficient light, it does not need a convex lens. To explore the benefits of lens-free operation, we measured the receiving angle of the solar panel using a rotating platform, as shown in Fig. 5(a). The laser beam was first perpendicular to the surface of the solar panel (corresponding to an angle of 0° in Fig. 5(b)) and then the solar panel was gradually turned clockwise (corresponding to positive angles in Fig. 5(b)) and counterclockwise (corresponding to negative angles in Fig. 5(b)), respectively. Note that the solar panel revolved around the central axis of the rotating platform instead of its own central axis. When the solar panel was gradually turned clockwise and counterclockwise, the LD shone on different areas of the solar panel. Fig. 5(b) illustrates the BERs of the 20.02-Mb/s 16-QAM OFDM signal over a 1-m air channel, when the solar panel is at different angles. We can see that the BERs are not symmetric, because different areas of the solar panel have different detection performances, as can be concluded from Fig. 4. It is due to the inherent property of the solar panel, which is originally not optimized for communication purpose. At the angles of −6° and 14°, the BERs are still below the forward error correction (FEC) limit of 3.8×10^{-3}. It can be calculated that the solar panel has a relatively large receiving angle (full angle) of around 20°. The solar panel with such a receiving area and a receiving angle has great potential to solve the problem of link alignment.

After some basic tests of the solar panel as discussed above, we began to investigate the feasibility of the solar panel-based UWOC. For the 16-QAM OFDM signal with 41 subcarriers, 32-QAM OFDM signal with 77 subcarriers and 64-QAM OFDM signal with 77 subcarriers, the achieved gross data rates were 20.02 Mb/s, 18.80 Mb/s, and 22.56 Mb/s, respectively, over a 7-m tap water channel. The corresponding net bit rates were 16.54 Mb/s, 15.53 Mb/s and 18.64 Mb/s, respectively, after removing the overheads of cyclic prefix (CP), FEC (7%), and training symbols. Fig. 6(a) and (b) are the waveform and spectrum of the 20.02-Mb/s 16-QAM OFDM signal. Fig. 6(c) is the spectrum of the 22.56-Mb/s 64-QAM OFDM signal. The gradual attenuation towards high-frequency subcarriers in the two spectra was ascribed to the limited bandwidth of the solar panel. The BERs curves of the 16-QAM/32-QAM/64-QAM OFDM signals versus received signal amplitudes are illustrated in Fig. 7. In the measurement, a neutral density filter put in front of the solar panel was used to change the optical power of the received signals, which indirectly changed the received signal amplitudes. Note that the receiving area of the power meter was smaller than the received light spot, and if a lens was used at the receiver side to focus the light spot into the receiving area of the power meter, the actual optical power could not be measured accurately. Therefore, we recorded the corresponding amplitude of the OFDM signal captured by the MSO. The insets present the constellation maps of the received 16-QAM/32-QAM/64-QAM OFDM signals with the BER of 1.6260×10^{-4}, 2.3377×10^{-3} and 3.5354×10^{-3}, respectively, which are well converged.

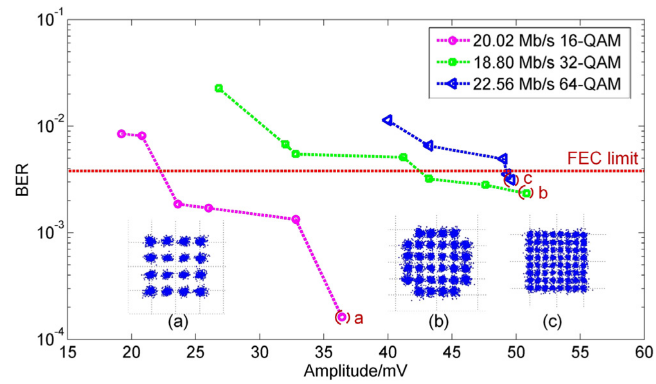

Fig. 7. BERs curves of the 16-QAM/32-QAM/64-QAM OFDM signals versus received signal amplitudes. Insets: constellation maps of the received 16-QAM/32-QAM/64-QAM OFDM signals with the BERs of 1.6260×10^{-4}, 2.3377×10^{-3} and 3.5354×10^{-3}, respectively.

Finally, we added different quantities of $Mg(OH)_2$ powders, which are commonly used as scattering agent for ocean optics research [2], into the water to investigate the impact of water turbidity on the solar panel-based UWOC. We measured the BERs of the 20.02-Mb/s 16-QAM OFDM signal versus $Mg(OH)_2$ concentration, as shown in Fig. 8. The insets show the corresponding constellation maps. With 0.086-mg/L $Mg(OH)_2$, the BER is 2.9268×10^{-3}, which is still below the FEC threshold of 3.8×10^{-3}. With 0.172-mg/L $Mg(OH)_2$, the measured BER (1.3008×10^{-2}) is above the FEC threshold due to reduced optical power at the solar panel, arising from the scattering and absorption of $Mg(OH)_2$ powders. The corresponding BERs versus different subcarriers is shown in Fig. 9.

4. Conclusion

In this paper, we have investigated the benefits of a self-powered solar panel, with large receiving area and lens-free operation, used as a detector in an UWOC system. The solar panel has a receiving area as large as ∼5 cm^2 and a receiving angle of around 20°, which

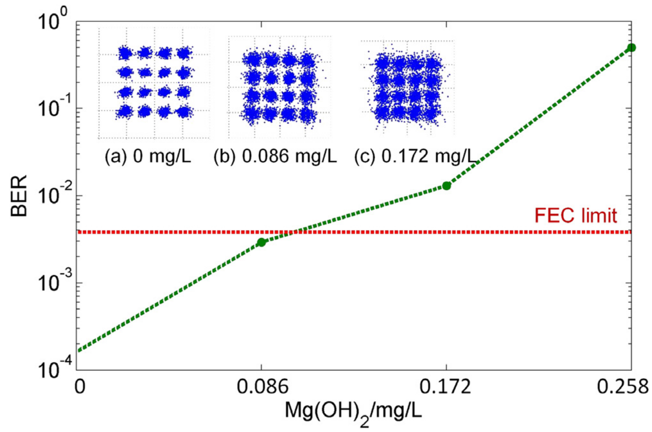

Fig. 8. BERs of the 20.02-Mb/s 16-QAM OFDM signal versus $Mg(OH)_2$ concentration. Insets: the corresponding constellation maps.

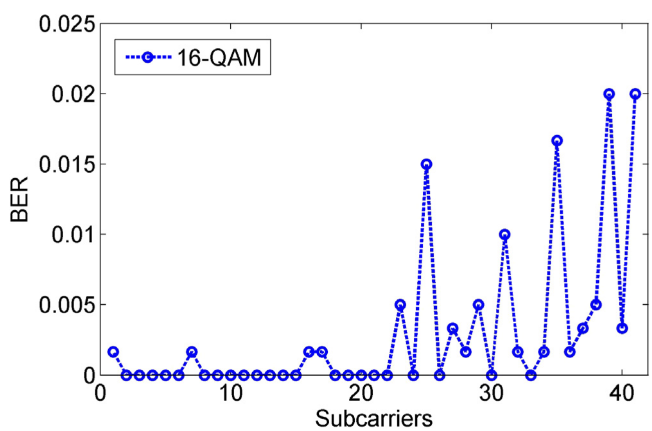

Fig. 9. With 0.086-mg/L $Mg(OH)_2$, BERs for different subcarriers.

can effectively relax the link alignment. Over a 1-m air channel, a data rate of 20.02 Mb/s is achieved using a 16-QAM OFDM signal within the receiving angle of 20°. Over a 7-m tap water channel, we acquire data rates of 20.02 Mb/s, 18.80 Mb/s and 22.56 Mb/s using 16-QAM, 32-QAM and 64-QAM OFDM signals, respectively. Finally, we investigate the impact of water turbidity on the solar panel-based UWOC by adding $Mg(OH)_2$ powders into the water. According to the presented results above, we can conclude that a solar panel with a large receiving area, lens-free operation and a dual function of data detection and energy harvesting has great potential for future self-powered underwater devices.

Acknowledgments

This work was supported in part by National Natural Science Foundation of China (NSFC) (61671409, 61301141), by National Key Research and Development Program of China (2016YFC1401202, 2017YFC0306601, 2017YFC0306100) and by Conservation Science and Technology Program of Administration of Cultural Heritage, Zhejiang Province (2016010).

References

[1] T.C. Wu, Y.C. Chi, H.Y. Wang, C.T. Tsai, G.R. Lin, Blue laser diode enables underwater communication at 12.4 Gbps, Sci. Rep. 7 (2017) 40480.

[2] Y. Song, W. Lyu, B. Sun, Y. Hong, F. Qu, J. Han, W. Zhang, J. Xu, Experimental demonstration of MIMO-OFDM underwater wireless optical communication, Opt. Commun. 403 (2017) 205–210.

[3] H.M. Oubei, R. Elafandy, K. Park, T.K. Ng, M.S. Alouini, B.S. Ooi, Performance evaluation of underwater wireless optical communications links in the presence of different air bubble populations, IEEE Photonics J. 4 (2017) 441–448.

[4] J. Baghdady, K. Miller, K. Morgan, M. Byrd, S. Osler, R. Ragusa, W. Li, B.M. Cochenour, E.G. Johnson, Multi-gigabit/s underwater optical communication link using orbital angular momentum multiplexing, Opt. Express 24 (9) (2016) 9794–9805.

[5] H.M. Oubei, J.R. Duran, B. Janjua, H.Y. Wang, C.T. Tsai, Y.C. Chi, T.K. Ng, H.C. Kuo, J.H. He, M.S. Alouini, G.R. Lin, S. Ooi Boon, 4.8 Gbit/s 16-QAM-OFDM transmission based on compact 450-nm laser for underwater wireless optical communication, Opt. Express 23 (2015) 23302–23309.

[6] Y. Chen, M. Kong, T. Ali, J. Wang, R. Sarwar, J. Han, C. Guo, B. Sun, N. Deng, J. Xu, 26 m/5.5 gbps air-water optical wireless communication based on an OFDM-modulated 520-nm laser diode, Opt. Express 25 (13) (2017) 14760.

[7] Z. Wang, D. Tsonev, S. Videv, H. Haas, On the design of a solar-panel receiver for optical wireless communications with simultaneous energy harvesting, IEEE J. Sel. Areas Commun. 33 (8) (2015) 1612–1623.

[8] W. Shin, S. Yang, D. Kwon, S. Han, Self-reverse-biased solar panel optical receiver for simultaneous visible light communication and energy harvesting, Opt. Express 24 (2016) A1300–A1305.

[9] S. Zhang, D. Tsonev, S. Videv, S. Ghosh, G.A. Turnbull, I.D.W. Samuel, H. Haas, Organic solar cells as high-speed data detectors for visible light communication, Optica 2 (7) (2015) 607–610.

[10] B. Malik, X. Zhang, Solar panel receiver system implementation for visible light communication, in: IEEE International Conference on Electronics, Circuits, and Systems, IEEE, 2016, pp. 502–503.

[11] R. Sarwar, B. Sun, M. Kong, T. Ali, C. Yu, B. Cong, J. Xu, Visible light communication using a solar-panel receiver, in: the 16th International Conference on Optical Communications and Networks (ICOCN 2017), 2017, pp. 1-3.

[12] R.C. Smith, K.S. Baker, Optical properties of the clearest natural waters (200–800 nm), Appl. Opt. 20 (2) (1981) 177–184.